

2012

Modeling the Dispersal of Eastern Oyster (*Crassostrea virginica*) larvae in Delaware Bay

Diego A. Narvaez
Old Dominion University

John M. Klinck
Old Dominion University, jklinck@odu.edu

Eric N. Powell

Eileen E. Hofmann
Old Dominion University, ehofmann@odu.edu

John Wilkin

See next page for additional authors

Follow this and additional works at: https://digitalcommons.odu.edu/ccpo_pubs



Part of the [Marine Biology Commons](#), and the [Oceanography Commons](#)

Repository Citation

Narvaez, Diego A.; Klinck, John M.; Powell, Eric N.; Hofmann, Eileen E.; Wilkin, John; and Haidvogel, Dale B., "Modeling the Dispersal of Eastern Oyster (*Crassostrea virginica*) larvae in Delaware Bay" (2012). *CCPO Publications*. 73.
https://digitalcommons.odu.edu/ccpo_pubs/73

Original Publication Citation

Narváez, D.A., Klinck, J.M., Powell, E.N., Hofmann, E.E., Wilkin, J., & Haidvogel, D.B. (2012). Modeling the dispersal of eastern oyster (*Crassostrea virginica*) larvae in Delaware Bay. *Journal of Marine Research*, 70(2-3), 381-409.

Authors

Diego A. Narvaez, John M. Klinck, Eric N. Powell, Eileen E. Hofmann, John Wilkin, and Dale B. Haidvogel

Modeling the dispersal of eastern oyster (*Crassostrea virginica*) larvae in Delaware Bay

by Diego A. Narváez^{1,2}, John M. Klinck¹, Eric N. Powell³, Eileen E. Hofmann¹,
John Wilkin⁴ and Dale B. Haidvogel⁴

ABSTRACT

The interactions of circulation and growth processes in determining the horizontal distribution of eastern oyster (*Crassostrea virginica*) larvae in the Delaware Bay estuary were investigated with a coupled circulation-individual-based larvae model that used environmental conditions from the spawning seasons (mid-June to mid-September) of 1984, 1985, 1986, 2000, and 2001. Particles, representing oyster larvae, were released at five-day intervals from areas in Delaware Bay that correspond to natural oyster reefs. The simulated larval development time was used to estimate potential larval success, determined by the percent of larvae that successfully reached settlement size (330 μm) within the planktonic larval duration of 30 days. Success rates for simulated larvae released in the upper estuary were less than half of those released in the lower estuary because of the reduction in growth rate from exposure to low salinity. Simulated larval success rates were further reduced during periods of increased river discharge, which produced low salinity conditions. The simulated transport patterns showed a down-estuary drift of oyster larvae during the spawning season, which is consistent with the observed reduction in settlement and recruitment rates in the upper estuary. The simulated transport pathways patterns showed that larvae originating in the middle and lower regions of the estuary had low rates of dispersion and high rates of self-settlement. Larvae released in the upper reaches of the estuary had limited contributions to the Delaware Bay oyster population, in part because of the lower overall simulated larval success in the low salinity regions. The simulated transport patterns suggested that the upper bay exports rather than receives larvae, which has implications for the establishment of genetic traits.

1. Introduction

The planktonic larval phase of the eastern oyster (*Crassostrea virginica*) typically lasts from 15 to 25 days (Kennedy, 1996). During this phase, oyster larvae swim upward on the flood tide in response to increased salinity and sink downwards on the ebb tide in response to decreased salinity (Carriker, 1951). Oyster larvae also have an ontogenetic migration

1. Old Dominion University, Center for Coastal Physical Oceanography, Department of Ocean, Earth and Atmospheric Sciences, Norfolk, Virginia, 23508, U.S.A.

2. Corresponding author. *email: diego@ccpo.odu.edu*

3. Rutgers University, Institute of Marine and Coastal Sciences and The New Jersey Agricultural Experiment Station, Haskin Shellfish Research Laboratory, Port Norris, New Jersey, 08349, U.S.A.

4. Rutgers University, Institute of Marine and Coastal Sciences, New Brunswick, New Jersey, 08901, U.S.A.

in which the young larvae (early stage, veliger) are in the upper water column and older larvae (late stage, pediveliger) are near the bottom (e.g., Carriker, 1951; Andrews, 1983). The transport of this nonuniform vertical larval distribution by the estuarine circulation potentially results in settlement of larvae in the spawning area or in areas that are away from the spawning location. The final settlement location is the result of circulation (passive transport), larval growth (determines planktonic duration), and behavior (active vertical movement) processes.

The oyster reefs in Delaware Bay (Fig. 1) cover a horizontal salinity gradient that ranges from about 5–10 in the upper estuary to 25–30 in the lower reaches of the estuary (Hofmann *et al.*, 2009). As a result, eastern oyster larvae originating from these reefs experience a salinity gradient as well as a gradient in food concentration (Powell *et al.*, this issue), both of which are important factors regulating growth and development (Dekshenieks *et al.*, 1993).

The comprehensive study of eastern oyster larvae presented in Carriker (1951) was developed around the premise that the horizontal distribution of the larvae directly affects the location of natural oyster reefs and the extent to which setting of oyster juveniles occurred on these reefs. Quantitative surveys of Delaware Bay oyster populations have been ongoing since 1953, which has allowed relationships between broodstock abundance and recruitment to be examined (Powell *et al.*, 2008). This analysis showed variability in recruitment to different parts of Delaware Bay and suggested that the frequency of good recruitment events increased down-estuary and that sporadic recruitment occurred on the Delaware side of the estuary. Thus, the larval source regions, the conditions that allow larvae to arrive at particular locations, and the controls exerted on larval growth at small as well as large scales interact to determine where and when larvae set. The degree of interaction among these many factors underlies the significant seasonal and interannual variations observed in recruitment to Delaware Bay oyster populations.

In this study the interactions of circulation and growth processes in determining the horizontal distribution of eastern oyster larvae in Delaware Bay were investigated with a circulation model coupled with an individual-based oyster larvae model. Specific research objectives focused on understanding variability in larval growth in response to along-estuary gradients in temperature and salinity, the dominant transport pathways, and the transfer of larvae between reef areas of Delaware Bay. These objectives are integral to the science goals of the Delaware Bay Ecology of Infectious Diseases initiative, which are focused on understanding how oyster populations in Delaware Bay respond to diseases, climate, and environmental and biological variability (Hofmann *et al.*, 2009).

The next section provides a description of Delaware Bay and the models used in this study. This is followed by descriptions of the simulations and results. The discussion and summary section places the simulation in the context of what is known about oyster distributions in Delaware Bay.

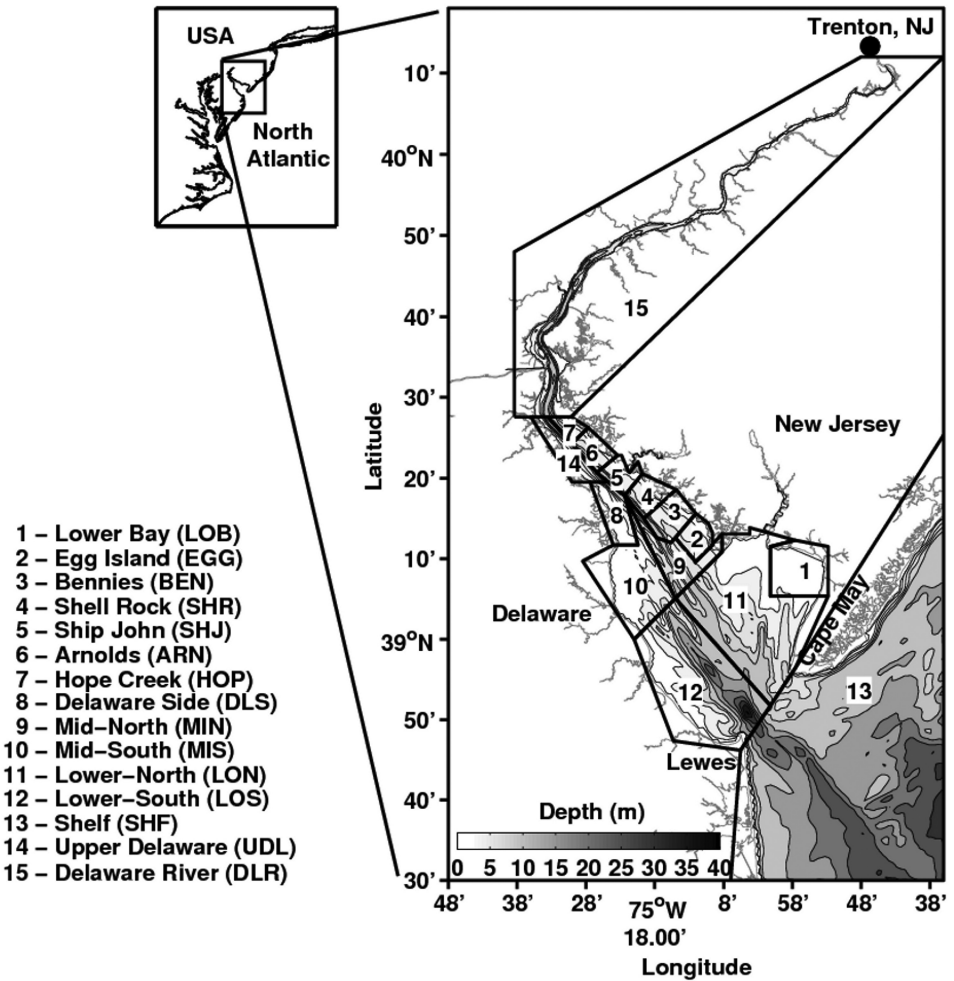


Figure 1. Map showing the location and bathymetry (shading) of Delaware Bay. The release areas for the simulated particles (areas 1–8) generally correspond to the locations of natural oyster reefs in Delaware Bay (see listing). These release areas and an additional seven regions (areas 9–15) were used to analyze the settlement patterns obtained from the Lagrangian particle tracking simulations. River discharge measurements were obtained from USGS gauges at Trenton, NJ.

2. Study area

The Delaware Bay, one of the larger estuaries in North America, is located on the United States eastern coast (Fig. 1). The estuary widens toward the ocean and is characterized by a main narrow channel along its center. Delaware Bay has an average depth of 12 m and is flanked by shoals with depths of 2–5 m (Fig. 1).

The Delaware River provides about 60% of the total freshwater that is discharged into the Delaware Bay (Sharp *et al.*, 1986). Mean monthly discharge measurements, obtained from the United States Geological Survey (USGS) water flow gauges for this river, show a seasonal cycle with maximum values of $580\text{--}630\text{ m}^3\text{ s}^{-1}$ during early spring (March and April) and minimum discharges of $170\text{--}175\text{ m}^3\text{ s}^{-1}$ during late summer and early autumn (August and September). Freshwater inputs from other rivers along the periphery of Delaware Bay provide the remaining 40% of the freshwater discharge.

In general, Delaware Bay waters are weakly stratified (Garvine, 1991; Garvine *et al.*, 1992) and the circulation consists of density-driven along-estuary flow on which is superimposed an across-estuary transverse flow that results from laterally varying bathymetry (Jacobsen *et al.*, 1990; Wong, 1994; Walters, 1997). The estuary circulation also has a wind-forced component (Wong and Garvine, 1984), which can weaken or enhance the two-layer estuarine flow (Galperin and Mellor, 1990). The Delaware Bay flow dynamics of interest for this study are described in Wang *et al.* (this issue).

Natural oyster reefs exist in the upper and middle portions of Delaware Bay (Powell *et al.*, 2008, encompassed by areas 2 to 7 in Fig. 1). Additional oyster reefs occur down-estuary of the natural reefs, mostly on grounds that are leased for commercial use (Fig. 1, areas 1 and 8, MacKenzie, 1996; Powell *et al.*, 1997; Kraeuter *et al.*, 2003). The higher salinity waters in the lower estuary enhance adult oyster growth; whereas, growth is reduced in lower salinity areas of the upper estuary (Kraeuter *et al.*, 2007). However, parasites that cause oyster diseases proliferate in the higher salinity regions, resulting in a trade-off between oyster growth and disease mortality (e.g., Haskin and Ford, 1982).

3. Circulation and larvae growth-behavior models

In this study, an individual-based oyster larvae growth-behavior model coupled to a circulation model was used to evaluate the relative effects of circulation (advection and diffusion), environmental conditions (temperature, salinity, food, turbidity), and biological processes (growth and swimming behavior) on oyster larvae dispersal patterns and primary transport pathways. The circulation model is described in detail by Wang *et al.* (this issue) and only a general description is presented here. The oyster larvae growth and behavior models are described in Dekshenieks *et al.* (1993, 1996, 1997) and the brief summary given below focuses on the linkages to the circulation and environmental conditions.

a. Circulation model

The hydrodynamic circulation model is based on the Regional Ocean Model System (ROMS) version 3.4 (www.myroms.org). This model is a free-surface, hydrostatic, primitive equations model that uses terrain-following coordinates (Shchepetkin and McWilliams, 2005). The model was configured and calibrated for the Delaware Bay and its adjacent continental shelf (Wang *et al.*, this issue). The domain consists of a curvilinear grid with horizontal resolution that ranges from $\sim 0.2\text{ km}$ in small areas (e.g., rivers) to $\sim 1.5\text{ km}$

on the continental shelf. Vertical processes are represented using sigma coordinates with 20 vertical levels with a resolution of ~ 0.03 m in shallow areas and ~ 6.2 m in deep areas. A 60-second time step was used for integration of the circulation fields. Details of the model configuration are given in Wang *et al.* (this issue).

External forcing of the circulation model included freshwater input from the six major tributaries of Delaware Bay estuary that was obtained from USGS water gauge measurements. The air-sea fluxes were estimated from distributions obtained from the North America Regional Reanalysis (Mesinger *et al.*, 2006). At the continental shelf open boundary, sea level and barotropic velocity were specified using outputs from a regional tidal model (Mukai *et al.*, 2002). Radiation conditions for the baroclinic velocity and tracers (e.g., temperature, salinity) were applied at the open boundaries (Marchesiello *et al.*, 2001). No additional temperature, salinity and velocity information was imposed at the boundaries. Initial conditions consisted of a flat sea surface, vertically uniform salinity with an along-estuary gradient that ranged from 10 in the upper estuary to 28 in the lower estuary, and a constant temperature of 6°C . The adjustment of the simulated fields from the initial conditions occurred in 2–3 days (Wang *et al.*, this issue). Model validation was done using observations of water level, temperature, and salinity from 2000 and temperature, salinity and currents observations from 2010–2011 as described in Wang *et al.* (this issue).

b. Eastern oyster larvae growth-behavior model

The oyster larvae growth and behavior models described in Deksheniaks *et al.* (1993, 1996, 1997) simulate the vertical and time-dependent distribution of the concentration of oyster larvae of a given size. For this study, the larval model was converted to an individual-based model so that the growth and swimming behavior of individual particles could be tracked.

i. Larval growth. The growth model simulates the time-dependent (t) change in larval size (SZ , $\mu\text{m d}^{-1}$) as a result of growth that is determined by food supply, the combined effects of temperature and salinity ($tsfactor$), and turbidity ($turbef$) as:

$$\frac{dSZ}{dt} = growth(food, size) \times tsfactor \times turbef. \quad (1)$$

Larval growth rate ($growth(food, size)$) was based on measured growth rates ($\mu\text{m d}^{-1}$) that were made at 28°C and a salinity of 26, for a range of food concentrations and oyster larvae sizes (Rhodes and Landers, 1973). These measurements were linearly interpolated to estimate growth rates for food concentrations of 0 to 6 mg C L^{-1} and larval sizes of 75 to $255\ \mu\text{m}$ (Fig. 2 of Deksheniaks *et al.*, 1993). The larval growth term in Eq. (1) is obtained from these values for a given food concentration and size. A temporally and spatially (horizontal and vertical) constant value of 4 mg C L^{-1} was used for the food concentration because data to specify a time and space varying food supply in Delaware Bay are lacking. Estimation of food concentration from environmental conditions (e.g., salinity) is not feasible because food concentration in Delaware Bay does not follow up- and

down-estuary trends in environmental gradients (Powell *et al.*, this issue). The constant food concentration used for the simulations is optimal for growth of eastern oyster larvae (Deksheniaks *et al.*, 1993). The food concentration remains fixed at 4 mg C L^{-1} throughout the simulations, i.e., it does not decrease as a result of consumption. The use of a constant optimal food supply removes this as a factor influencing larval growth, allowing the effects of temperature and salinity to be determined.

The food- and size-dependent growth rate was scaled using oyster larvae growth rates measured at a range of temperature and salinity values (Davis, 1958; Davis and Calabrese, 1964). These growth rates were linearly interpolated to obtain values for temperatures between $18\text{--}32^\circ\text{C}$ and salinities between $7.5\text{--}27.5$ (Fig. 3 of Deksheniaks *et al.*, 1993). The interpolated growth rates were normalized by the food and size-dependent rate (28°C , salinity 26) so that the *tsfactor* in Eq. (1) is nondimensional. For a given temperature and salinity, this factor gives the fractional increase or decrease in larval growth rate relative to the base rate.

The effect of turbidity (*turbef* in Eq. 1) on larval growth rate was obtained from laboratory studies on hard clam (*Mercenaria mercenaria*) larvae (Davis, 1960) and adapted for eastern oyster larvae (Deksheniaks *et al.*, 1993; 1996; 1997). At turbidity concentrations below $0.1 \text{ g dry wt L}^{-1}$ larval growth is enhanced, and Deksheniaks *et al.* (1993; 1997) expressed this turbidity effect (*turbef*) as:

$$turbef = m \times turb + c, \quad (2)$$

where *turb* is the ambient turbidity concentration (g dry wt L^{-1}), and *m* and *c* are $0.542 (\text{g dry wt L}^{-1})^{-1}$ and 1.0, respectively. The relationship given by Eq. (2) gives the fractional increase in larval growth rate for turbidity concentrations between 0 and $0.1 \text{ g dry wt L}^{-1}$. For turbidity concentrations greater than $0.1 \text{ g dry wt L}^{-1}$, larval growth is reduced and Deksheniaks *et al.* (1993; 1997) expressed this fractional decrease as:

$$turbef = be^{-\beta(turb-turb0)}, \quad (3)$$

where *b*, β and *turb0* are 0.375, 0.5 (g dry wt L^{-1})⁻¹ and $2.0 \text{ g dry wt L}^{-1}$, respectively. Turbidity measurements from Delaware Bay are insufficient to provide time and space varying fields for the larval model. Additionally, the turbidity effect on larval growth is small (Deksheniaks *et al.*, 1993) so ambient turbidity concentration was set to zero, i.e., *turbef* = 1, over the estuary for all time, which removes the turbidity effect.

ii. *Larval behavior*: The vertical velocity of each larva (W_{bio} , mm s^{-1}) was obtained from the relationship given in Deksheniaks *et al.* (1996) which is based on the fraction of time spent swimming (*TS*, nondimensional), a temperature and size-dependent vertical swimming rate (*SW*, mm s^{-1}), and a size-dependent sinking rate (*SR*, mm s^{-1}) as:

$$W_{bio} = TS \times SW - (1 - TS) \times SR. \quad (4)$$

The swimming rate (SW) was obtained from laboratory measurements of the vertical displacements of eastern oyster larvae of different sizes for a range of temperatures (e.g., Hidu and Haskin, 1978), which were used to develop temperature and size-dependent swimming rates (Fig. 2 of Deksheniaks *et al.*, 1996). The derived vertical swimming rate increases with increasing temperature and the rate of this increase varies with larval size.

Larval sinking rate (SR) increases with increasing larval size, and Deksheniaks *et al.* (1996) used measurements given in Hidu and Haskin (1978) to derive a relationship of the form:

$$SR = SR_0 e^{c(SZ-SZ_0)}, \quad (5)$$

where SR_0 is 2.665 mm s^{-1} , c is $0.0058 \mu\text{m}^{-1}$, SZ is larval size (μm) and SZ_0 is $220 \mu\text{m}$. Larval sinking rate increases with increasing larval size (Fig. 3 of Deksheniaks *et al.*, 1996).

Oyster larvae combine periods of upward motion with periods of rest (e.g., Hidu and Haskin, 1978) and observations suggested that the percent of time that oyster larvae swim is a response to time-varying changes in salinity (Kennedy and Van Heukelem, 1986). Deksheniaks *et al.* (1996) used these observations to derive a relationship for the fraction of time that the larva swims (TS) of the form:

$$TS = d1 \times \Delta S + d2, \quad \text{for increasing salinity} \quad (6)$$

and

$$TS = -d3 \times \Delta S + d4, \quad \text{for decreasing salinity}, \quad (7)$$

where ΔS is the salinity change in time ($\text{salinity time}^{-1}$) and $d1$ and $d3$ are 0.0622 and $0.0668 (\text{time } \Delta S)^{-1}$, respectively, and $d2$ and $d4$ are 0.3801 and 0.7515 , respectively.

c. Coupled circulation-larvae model

The ROMS framework includes a range of capabilities, one of which is a particle tracking module that uses the time- and space-dependent advective velocity field, $\vec{U}(\vec{X}, t)$ to estimate the change in the location of a particle along a three-dimensional (x, y, z) trajectory given by \vec{X} based on the governing equation for Lagrangian motion as:

$$\frac{d\vec{X}}{dt} = \vec{U}(\vec{X}, t) + W_{vw}\hat{Z} + W_{bio}\hat{Z}. \quad (8)$$

The particle location is also modified by sub-grid vertical mixing ($W_{vw}\hat{Z}$), which is included as a random vertical displacement, W_{vw} . The amplitude of the vertical random motion is based on the vertical temperature diffusivity and a normally distributed random term of zero mean and unit variance (Hunter *et al.*, 1993; Visser, 1997). The random vertical displacement is added to the vertical particle location (\hat{Z}) at each time step. The particle location at each time is obtained using a 4th order Milne-predictor/Hamming-corrector numerical integration

scheme (Hamming, 1959). The particle-tracking module also interpolates the temperature and salinity obtained from the circulation model to each particle location.

The oyster larval model was coupled to the circulation model by modifying the ROMS particle-tracking module to calculate the time-dependent change in larval size (dSZ/dt , Eq. 1) along the trajectories and to include vertical displacement due to the larval swimming or sinking behavior, $W_{bio}\hat{Z}$ (Eq. 3). The larval model runs simultaneously with the circulation model using the information estimated by the particle tracking module (i.e., particle location, vertical random walk, temperature and salinity) at each time step (60-seconds). The trajectory for each larval particle was ended when the simulated larva reached settlement size ($330\ \mu\text{m}$, Deksheniaks *et al.*, 1993) or did not develop to settlement size within 30 days. The oyster larvae model has been embedded in the circulation model and it is available as a capability of ROMS.

4. Simulations

a. Simulation design

Particles were released at areas that correspond to the existing natural oyster reefs in the upper and middle portions of Delaware Bay (areas 2 to 7, Fig. 1). Additional release areas were in the lower Delaware Bay (area 1, Fig. 1) and along the Delaware side (area 8 in Fig. 1) where less extensive oyster reefs exist. Particles were released at 40 locations evenly distributed within each release area (areas 1 to 8, Fig. 1). At each of the 40 locations, 5 particles were released, giving a total of 200 particles released in each area. Each particle was released from $\sim 0.2\text{--}0.5$ m above the bottom. The 200 particles were simultaneously released at midnight from each area, which made the release time independent of the tidal phase. The releases were repeated at five-day intervals from mid-June to mid-September, which encompasses the spawning period of eastern oyster larvae in mid-latitude estuaries, such as Delaware Bay (Thompson *et al.*, 1996). Thus, 18 spawning events were simulated in each area, resulting in a total of 28,800 particles (1600 per spawning event) released over the entire season. The release areas used for the simulations do not account for the irregular shapes and variable oyster densities of the natural oyster reefs. Thus, the particle releases provide a general view of transport to and from these areas.

For analysis of the Lagrangian particle trajectories, Delaware Bay was sub-divided into fifteen regions (areas 1 to 15, Fig. 1). These regions include the release areas (areas 1 to 8, Fig. 1), as well as areas where oyster reefs are less well established or not found (areas 9 to 15, Fig. 1). The latter regions allow analysis of potential regions where oyster larvae may settle but not necessarily survive.

Simulations were done using environmental conditions from the spawning seasons of 1984, 1985, 1986, 2000, and 2001. These years include the effects of high (1984, 2000) and low (1985, 2001) river discharge on oyster larvae transport and survival. Environmental conditions in 1986 were representative of intermediate conditions in Delaware Bay. Observations that can be used to evaluate the Lagrangian simulations were available for each of these years.

The sensitivity of the simulation results to an optimal constant food supply (4 mg C L^{-1}) and no turbidity (0 g L^{-1}) was assessed by redoing the simulations for the spawning season of 2000 using modified food and turbidity concentrations. The food supply was reduced by 50% (2 mg C L^{-1}) and turbidity was increased to 0.2 g L^{-1} , which is an average value measured for the upper-middle Delaware estuary (Cook *et al.*, 2007). The modified food supply and turbidity were held constant in time and space. The influence of size at settlement was examined by allowing the larva to set at smaller sizes of $270 \mu\text{m}$ and $300 \mu\text{m}$.

b. Lagrangian trajectory analysis

In mid-latitude systems, such as the Delaware Bay, eastern oyster larvae typically reach settlement size within 30 days (Kennedy, 1996). Thus, simulated larval success was defined as the percent of the total released larvae that developed to settlement size within 30 days. This value was calculated for each particle originating in the release areas (8 sites) for each spawning event (18 release times). The along-trajectory temperature and salinity values encountered by the successful larvae were averaged to obtain the mean environmental conditions.

Spearman rank correlations were used to determine statistical dependence between larval success and the average temperature and salinity encountered along a trajectory and between river discharge and encountered salinity for the different release locations for the five years. A one-way analysis of variance (ANOVA) was used to test for statistically significant differences in the temperature and salinity encountered along the particle trajectories and in larval success for particles originating in the different release areas for the five years included in the study. The significance levels for the ANOVA were estimated using the effective degrees of freedom which represent the number of independent estimates in a time series as determined from lagged correlations (Emery and Thomson, 2001).

The transfer of oyster larvae among the different regions of Delaware Bay was examined using connectivity matrices, which show the percent of larvae arriving at a particular location in terms of the total larvae that were released at another location. The matrices were based on only the larvae that reached settlement size within 30 days and provide a view of possible settlement regions. The connectivity matrices indicate potential settlement areas because the simulations do not include water column planktonic mortality (e.g., predation), cues that trigger larval settlement, or post-settlement mortality. Connectivity matrices were calculated for all five years and for the sensitivity simulations and compared to determine changes in larval success and transport.

c. Delaware Bay oyster data sets for model evaluation

Measurements of oyster larvae settlement and recruitment were made at 30–35 sites distributed throughout the New Jersey and Delaware portions of Delaware Bay at yearly intervals from 1954 to 1986 (sampling details in Fegley *et al.*, 2003 and Powell *et al.*, 2008). Settlement counts were collected for the spawning season in each year using wire mesh bags,

which were suspended just above the bottom and contained clean oyster shells. The shell bags were replaced every week between late June and the end of August and every two weeks until early October. Each shell was examined under a microscope to count the newly settled oyster (spat) and age estimates of the spat were used to determine settlement time. The mean number of spat per shell was calculated for each location; the means of each shell bag that was replaced at each location were summed to obtain the mean cumulative spat count per shell for each spawning season. The means from the sampling sites for all years were used to obtain a long-term pattern of the oyster larvae settlement in Delaware Bay.

Annual oyster surveys in the New Jersey waters of Delaware Bay have been ongoing from 1953 to present (Powell *et al.*, 2008) and these data provide estimates of oyster recruitment determined from the ratio of spat (newly settled larva) to adult (oyster > 1-yr). The recruitment data were divided into four bay groups that included several oyster reefs, which were defined by the long-term average rates of adult oyster mortality, productivity, and the efficiency of the gear used in the surveys (see Powell *et al.*, 2008 for details). The observed mean recruitment data for 1984, 1985, 1986, 2000, and 2001 that correspond to the low, medium upbay, medium downbay, and high mortality groups were used to evaluate the simulated potential settlement patterns. The comparison with observations was done using the percent of the total simulated larvae that settled at Arnolds, Ship John, Shell Rock and Bennies, areas that correspond to the regions used to estimate observed recruitment rates (Table 1). The model-derived potential settlement estimates are not equivalent to the observed recruitment rates because they do not account for larval and post-settlement mortality and variable food supply effects, for example. Therefore, comparisons with the model-derived estimates are in terms of trends, and differences with observed recruitment values may provide indications of the importance of planktonic, post-settlement, and environmental effects.

5. Results

a. Environmental effects on larval growth and success

The distribution of particles released in the upper, middle and lower portions of the Delaware Bay provided general trends in larval growth and success that resulted from spatial and temporal variability in the temperature and salinity distributions (Fig. 2). Ten days after release, larvae originating in the low salinity (salinity less than 10) region (Hope Creek, Fig. 2a) were half the size of those released in the higher salinity Lower Bay region (Fig. 2c). Larvae released in the mesohaline central portion of the estuary (Shell Rock) were of intermediate size (Fig. 2b). After 20 days, differences in larval size in the three salinity zones were more pronounced (Fig. 2d–f). Larvae that remained in the upper-most part of the estuary were $\sim 100 \mu\text{m}$ smaller than those just a few kilometers down estuary (Fig. 2d–f). Larvae released in the Lower Bay that remained in the warmer and higher salinity waters along the New Jersey side of the estuary were larger than those that moved to the center of the lower estuary (Fig. 2f) and were considerably larger than those in the upper estuary

Table 1. Observed recruitment, expressed as the ratio of spat to adult oyster, measured for reef groups in Delaware Bay that were defined based on adult oyster mortality (see Table 1 of Powell *et al.*, 2008) for the five years used for the Lagrangian simulations. The mean recruitment for each year and group was calculated from the measurements. Also shown are the percent of the total larvae released in the simulations that successfully reached settlement size that were calculated for similar-sized areas. The observed (spat/adult ratio) and simulated (potential settlement) values are different metrics and are not comparable in terms of magnitude; only trends should be compared.

Year	Low mortality	Medium upbay mortality	Medium downbay Mortality	High mortality	Mean
Observed recruitment (spat/adult ratio)					
1984	0.002	0.03	0.04	0.08	0.04
1985	0.09	0.69	1.21	1.30	0.82
1986	1.16	5.08	10.73	2.33	4.83
2000	0.15	0.2	0.79	1.08	0.56
2001	0.05	0.09	0.22	0.44	0.20
Mean	0.29	1.22	2.59	1.05	
Simulated potential settlement					
	Arnolds	Ship John	Shell Rock	Bennies	
1984	4.91	2.26	5.49	3.42	4.02
1985	4.80	2.71	5.73	4.82	4.51
1986	4.80	2.83	6.51	4.59	4.68
2000	3.84	2.55	7.82	4.02	4.56
2001	4.16	2.74	5.54	3.77	4.05
Mean	4.50	2.62	6.22	4.13	

regions. At 30 days, the larvae released in the upper estuary remained small (Fig. 2g) and had not reached settlement size. Most of the larvae released in the mid and lower regions reached settlement size (Fig. 2h, i).

The larvae released at Shell Rock in the mid-reaches of Delaware Bay (Fig. 2b) were broadly dispersed; whereas, those released at the Hope Creek and Lower Bay sites were less dispersed (Fig. 2a, c). Comparison of the larvae dispersion against the average conditions of temperature and salinity during the same period suggests that larvae that stayed in waters with higher temperatures and salinity developed faster than larvae that stayed in low temperature and low salinity waters (Fig. 2j, k).

The average temperature and salinity encountered by successful larvae along their trajectories was calculated for each release time and area for each of the five years (Fig. 3a,b) and compared to the percentage of larvae that successfully reached a competent size to settle within 30 days (larval success) (Fig. 3c). The temperature encountered by the larvae was typically above 18°C throughout the spawning season in all years, but periods with temperature above 20°C varied between the years (Fig. 3a). In 1984, larvae encountered cool temperatures until mid-July and again in late August. The spawning season in 1986 was characterized by a short period of temperatures above 22°C that extended throughout the

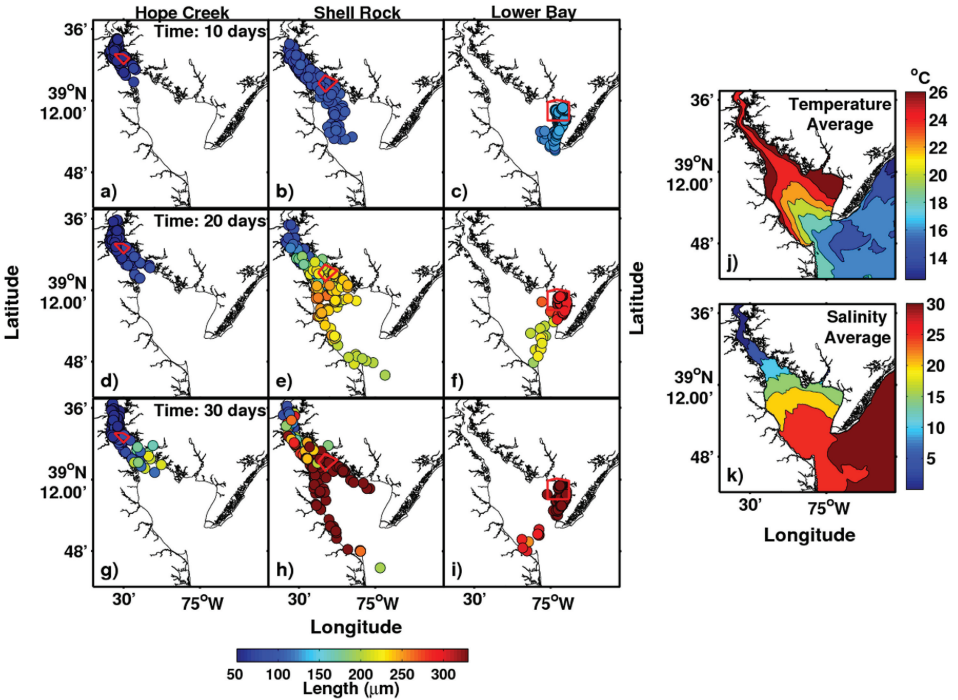


Figure 2. Dispersion and development, indicated as length, distribution for simulated larval particles at 10 days (a–c), 20 days (d–f), and 30 days (g–i) post release from 15 June 2000. Particle release areas (red outlined area) correspond to low (Hope Creek, a, d, g), moderate (Shell Rock, b, e, h) and high (Lower Bay, c, f, i) salinity conditions. The 30-day depth-averaged (j) temperature and (k) salinity distribution corresponding to the release date are shown.

estuary. During 2000 and 2001, water temperatures warmed above 18°C early in the spawning season and remained consistently warm throughout the estuary until mid to late August.

The salinity encountered by larvae was greater than 20 in the lower reaches of Delaware Bay and decreased to values less than 12 in the upper estuary (Fig. 3b). Over a spawning season, maximum salinity occurred in August and September in the lower to mid-regions of the estuary. The differences in salinity during the spawning seasons of the five years were most pronounced in June and early July. In the early part of the 1984, 1985, and 2000 spawning seasons, larvae released at Shell Rock, Bennies, and Egg Island encountered salinities less than 20 (Fig. 3b), which is below the value for optimal growth (Deksheniaks *et al.*, 1993).

The percentage of successful larvae was higher during mid-July and mid-August, when maximum temperatures occurred (Fig. 3a,c). Spearman rank correlations between the average temperature (Fig. 3a) and the simulated larval success (Fig. 3c) were low, but statistically significant for all years (Table 2). Larvae released from the Lower Bay and Egg

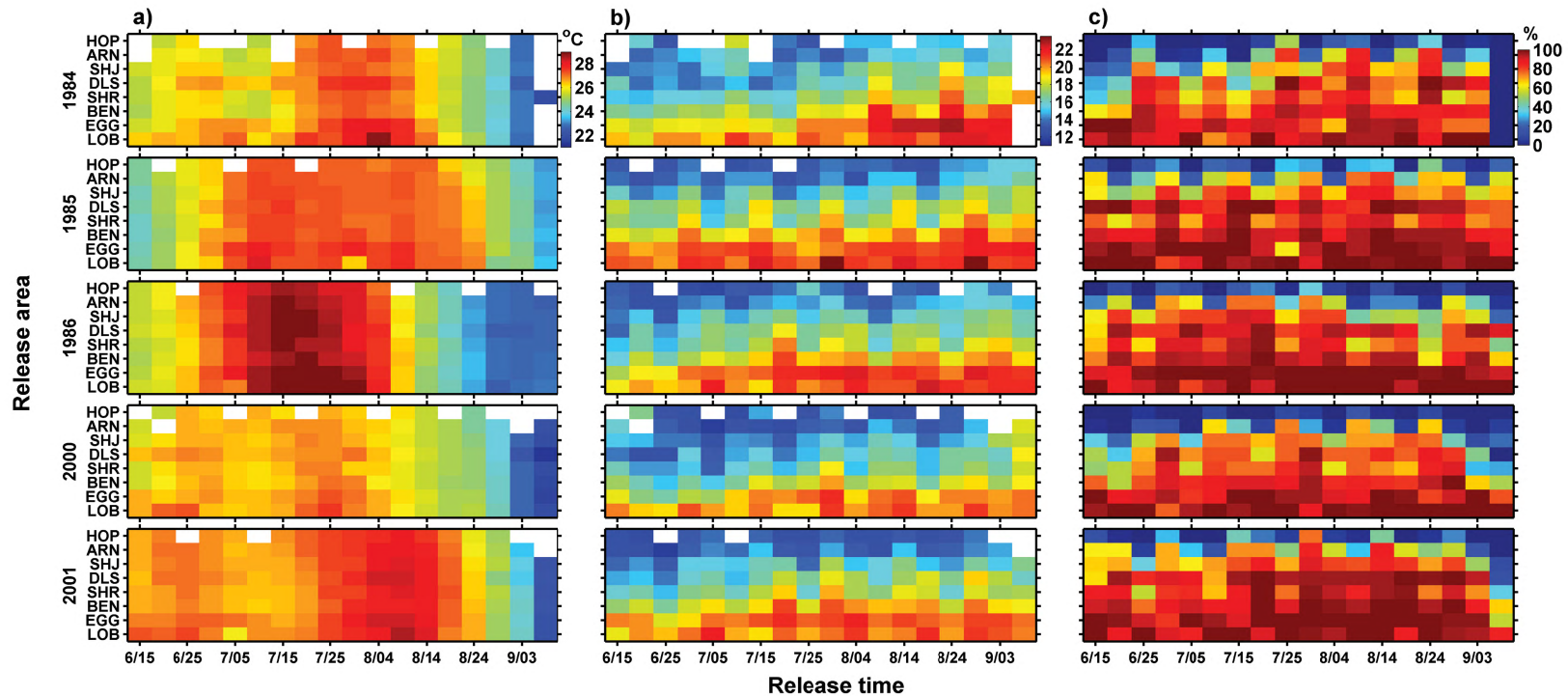


Figure 3. The distribution of the average (a) temperature and (b) salinity encountered by successful larvae along the particle trajectories and (c) simulated larval success for each release area and release time for each of the simulation years. Average temperature and salinity could not be calculated for areas and times when larval success was zero (white regions in (a) and (b)).

Table 2. Spearman rank correlations calculated between simulated larval success and the average temperature and average salinity encountered along the particle trajectories for each simulation year. Larval success was determined by the number of the simulated larvae reaching 330 μm in 30 days relative to the total number released. Temperature, salinity and larval success data are shown in Figure 3. All correlations are significant ($p < 0.05$).

	1984	1985	1986	2000	2001
Larval success vs. temperature	0.24	0.21	0.21	0.20	0.27
Larval success vs. salinity	0.68	0.84	0.85	0.74	0.80

Island regions (locations on Fig. 1) had high simulated success rates (Fig. 3c). Larval success decreased toward the upper estuary, with larvae released from Hope Creek having the lowest potential success rate for any spawning season. The down-estuary increase in larval success was associated with the down-estuary salinity gradient (Fig. 3c), as indicated by the significant Spearman rank correlations between salinity and larval success (Table 2). The higher correlations between larval success and encountered salinity suggest that salinity may be more important than temperature in determining larval success.

The mean water temperature encountered by larvae was similar for each release area in all years (Fig. 4a). The mean encountered salinity was similar for particles released from the individual release areas (Fig. 4b). However, the mean encountered salinity increased from about 13–14 at Hope Creek to about 20 in the Lower Bay (Fig. 4b). Mean larval success was similar for the individual release areas for each year, but showed a down-estuary trend, with the lowest values at Hope Creek in the upper estuary and highest values in the Lower Bay (Fig. 4c). The one-way ANOVA test showed that the mean values at the individual release areas for the five spawning seasons were not statistically significant. However, the along-estuary variability in salinity and larval success was statistically significant between the upper estuary regions (Hope Creek, Arnolds) and the middle-lower regions (Bennies-Lower Bay). Along-estuary variations in temperature and larval success were not statistically significant.

The Delaware River discharge was averaged for the 30 days following the larvae release date (Fig. 5) and compared with the average salinity conditions encountered by the larvae for each year. The 30-day mean river discharges showed year-to-year variations in the magnitude and timing of high river discharge events (Fig. 5). The highest river discharge occurred at the beginning of the spring-summer period, with the exception of 1985 when high discharge occurred at the end of the spawning season (Fig. 5). Lower salinity was encountered early in the 1984, 1986, and 2000 spawning seasons (Fig 3b), coinciding with the periods of high river discharge for the same years, especially for 1984 and 2000 (Fig. 5). However, Spearman rank correlations between encountered salinity and river discharge were not significant for most years and release areas, with the exception of some release locations in 1984, 1986, 2000, and 2001 (Table 3). The lack of significant correlations may result from the low variability and low river discharge during the summer in most years (Fig. 5).

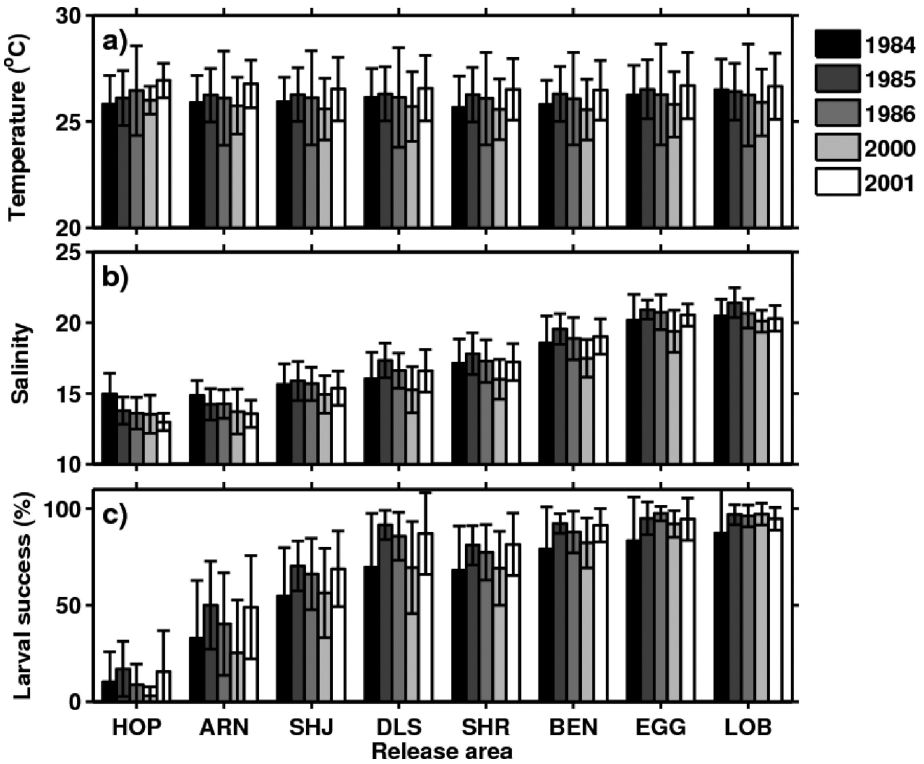


Figure 4. Means and standard deviations calculated from encountered (a) temperature, (b) salinity, and (c) simulated larval success for particles released in the indicated areas (locations given in Fig. 1) between mid-June and mid-September for each simulation year (time series data shown in Fig. 3). Larval success was determined by the number of larvae reaching $330\ \mu\text{m}$ in 30 days relative to the total number released. An analysis of variance (one-way ANOVA) showed that the temperature, salinity, and larval success means calculated for each release area were not statistically different between years. The effective degrees of freedom estimated for each release area for temperature (38–41), salinity (30–50), and larval success (65–70) were based on decorrelation scales of 10–15 days for temperature and salinity and 5–10 days for larval success.

b. Larval dispersion

The simulated larvae often reached a competent size to settle over the shoals and in the upper and northern region of the lower estuary (Fig. 6). Few of the simulated larvae potentially settled in the center of the lower estuary, and almost no larvae were exported to the adjacent continental shelf. This general pattern occurred in all years, with little variability between years.

The dispersal of oyster larvae between areas of Delaware Bay was determined using connectivity matrices that were calculated as the percent of the total larvae released at each area during the spawning season (200 particles, 18 releases, total 3600 particles) that reached a competent size to settle within each settlement region (Fig. 1). The connectivity

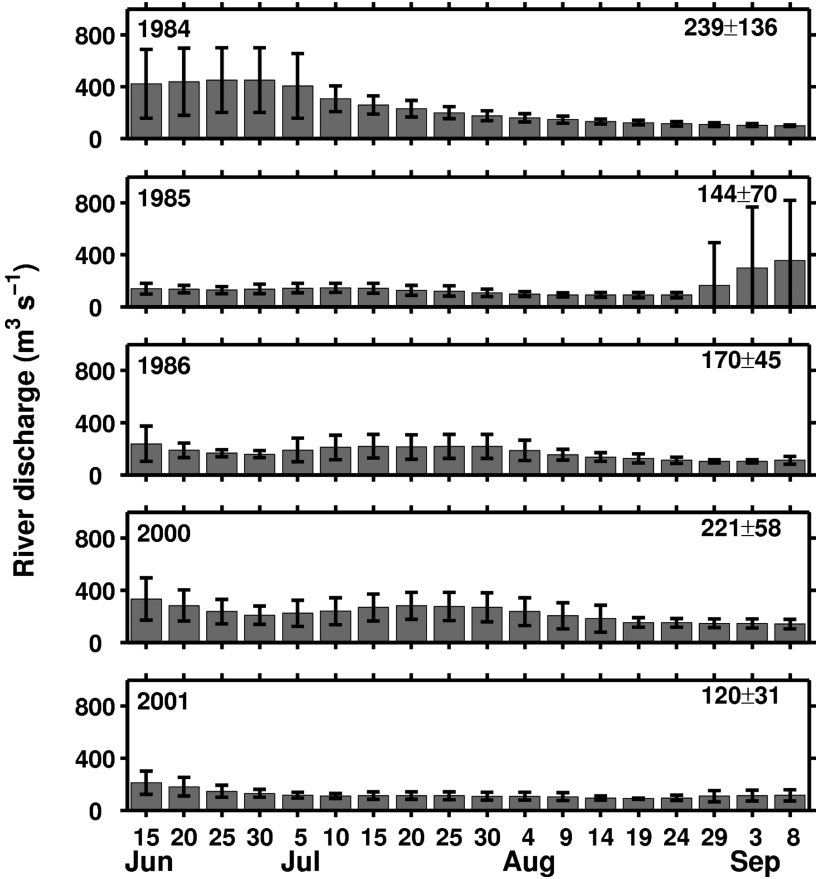


Figure 5. Thirty-day average and standard deviation calculated for river discharge for each release time during the oyster spawning season for the five years used in this study. The average and standard deviation for the river discharge for each spawning season is indicated.

Table 3. Spearman rank correlations between average salinity encountered along the particle trajectories and river discharge (data in Fig. 3b and Fig. 5) for particles released from the indicated oyster reefs (areas on Fig. 1) for each simulation year. Significant correlations are indicated by bold text ($p < 0.05$).

Year	HOP	ARN	SHJ	DLS	SHR	BEN	EGG	LOB
1984	-0.15	-0.40	-0.76	-0.83	-0.86	-0.83	-0.85	-0.74
1985	0.39	0.34	0.33	0.10	0.23	-0.03	0.34	-0.08
1986	-0.05	-0.36	-0.23	-0.09	-0.16	-0.24	-0.26	-0.56
2000	0.47	-0.31	-0.36	-0.69	-0.41	-0.26	-0.25	-0.40
2001	-0.08	-0.30	-0.30	-0.62	-0.48	-0.55	-0.50	-0.32

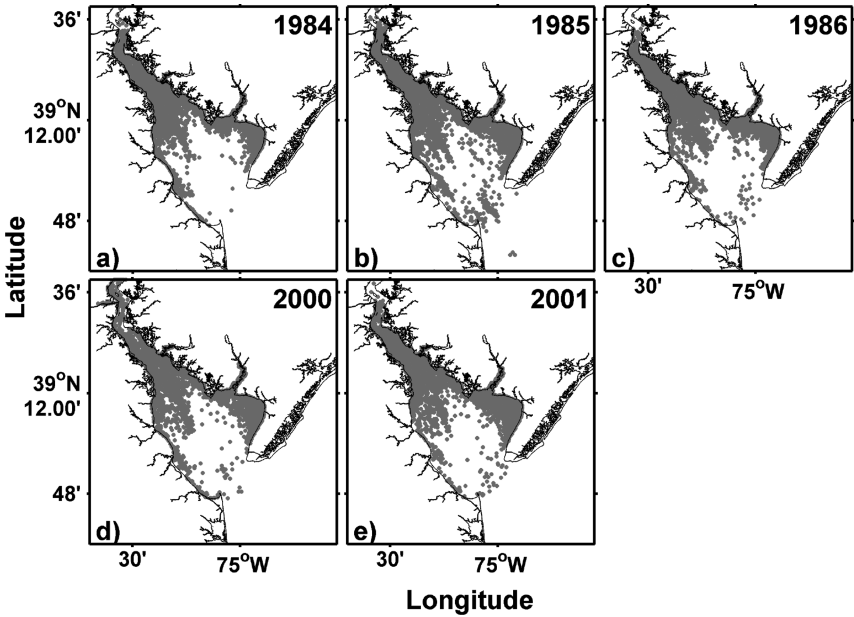
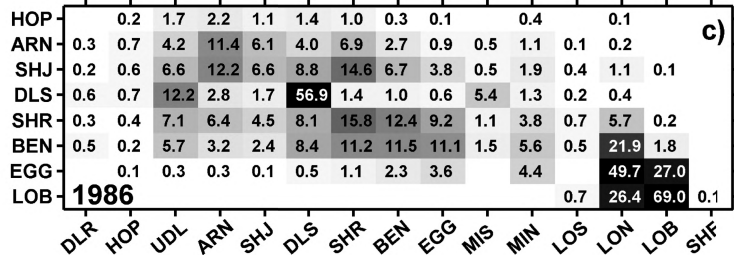
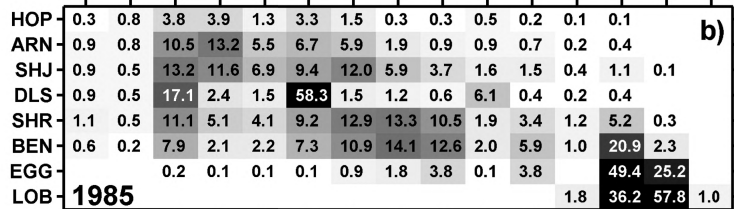
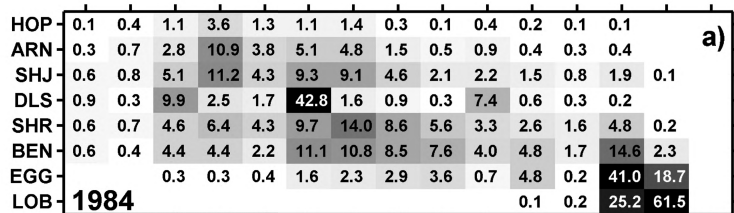


Figure 6. Distribution of potential settlement locations for all successful larvae released in the spawning seasons of (a) 1984, (b) 1985, (c) 1986, (d) 2000, and (e) 2001.

matrices provided estimates of larval transfer between different regions of Delaware Bay and of potential settlement of larvae in each region. The general larval dispersion pattern was similar in each year, but the magnitude of the transfers varied from year to year (Fig. 7).

The lowest larval exchanges occurred in the upper reaches of Delaware Bay (e.g., Hope Creek) where fewer than 5% of the total released larvae reached settlement size within 30 days in any of the settlement areas (Fig. 7). A portion of the successful larvae originating in the Hope Creek region were transported down-estuary and settled at Arnolds in the upper estuary and Ship John in the central estuary (Fig. 7). Larvae originating at Arnolds and Ship John tended to remain in the surrounding regions with about 10% settling at their origination site (Fig. 7). These sites also exported a large percentage of larvae down-estuary as far as Egg Island (Fig. 7), and also exported less than 1% of larvae up-estuary. Similar results occurred for larvae released from Shell Rock and Bennies (Fig. 7). Simulated larvae originating in the Egg Island region had fewer than 5% settlement at the same site or at any other adjacent oyster reef sites for any of the five years. The majority of the larvae were exported down-estuary, with more than 50% of the initial larval pool reaching settlement size in the Lower-North and Lower Bay regions (Fig. 7). The Lower Bay region received small inputs of larvae from the middle portions of Delaware Bay in any particular year (<0.2%) and no inputs from the upper estuary regions. Larvae released in the Lower Bay mostly remained in the region. Larvae originating in this region had no potential to settle



Settlement area

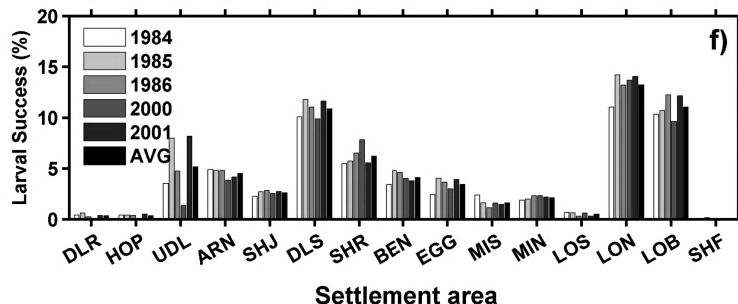
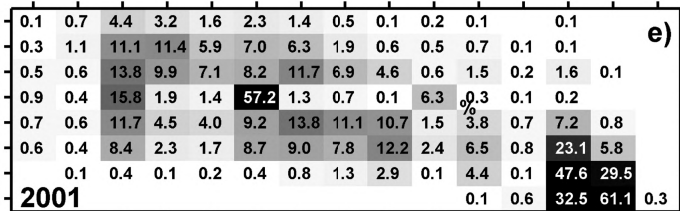
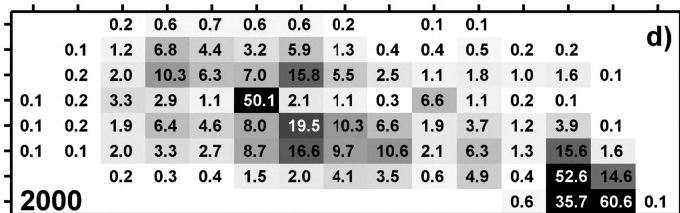


Figure 7. The percent of total larvae released in a particular area (y axis) that successfully settled in the same or another area (x axis) calculated from the particle trajectories obtained for (a) 1984, (b) 1985, (c) 1986, (d) 2000, and (e) 2001. The degree of connectivity is indicated by the shading and values less than 0.05% are indicated by white shading. (f) The percent of the total larvae released from all release areas and all release times that settled in each location for each year and the five-year average (AVG).

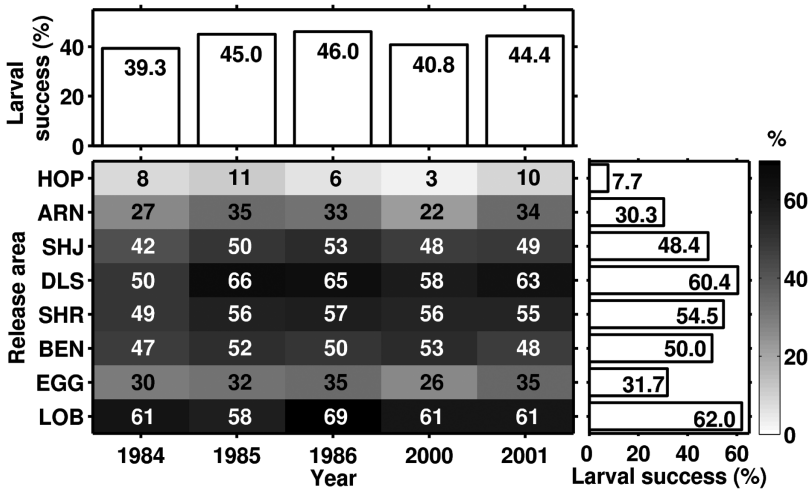


Figure 8. Percent of total larvae that successfully settled only on the natural oyster reefs in each year, compared to the average larval success for each year (upper panel) and the five-year average success for each area (right panel).

in the upper and middle estuary regions. Of the natural oyster reefs, Hope Creek and Egg Island showed low rates of potential self-settlement (i.e., larvae settling in the same area where they were released) and received small inputs from other regions of Delaware Bay. Larvae originating in these regions tended to be exported to others areas. The reef areas along the Delaware Side of the estuary and Lower Bay regions showed high rates of potential self-settlement (>40%).

The variability in potential larval settlement for the five years was estimated as the percent of all the released larvae that reached settlement size in any of the settlement areas (Fig. 7f). These percentages showed that rates for 1984 and 2000 were lower than those for the other years, particularly for the Upper Delaware, Ship John, Delaware Side, Bennies, Egg Island and Lower Bay regions. These years also had lower larval success.

Larvae reaching settlement size in areas other than the release areas (natural oyster reefs) potentially represent losses for the Delaware Bay oyster population because these areas generally lack suitable substrate for settlement. Therefore, the percent of the total released larvae that potentially settled in the natural oyster reef areas (areas 1 to 7, Fig. 1) was calculated for each year as an estimate of the relative contribution of larvae to only the Delaware Bay oyster populations (Fig. 8). The spawning season average (upper panel in Fig. 8) and release area average (right panel in Fig. 8) correspond to the average larval success per year and release areas, respectively. These values suggest that 40–45% of the simulated oyster larvae particles released in Delaware Bay could potentially settle on a natural reef (upper panel, Fig. 8). The Hope Creek reef region had the lowest success rate, 8–11%, with an overall average of 7.7% (right panel, Fig. 8). The reef areas between Ship John and Bennies

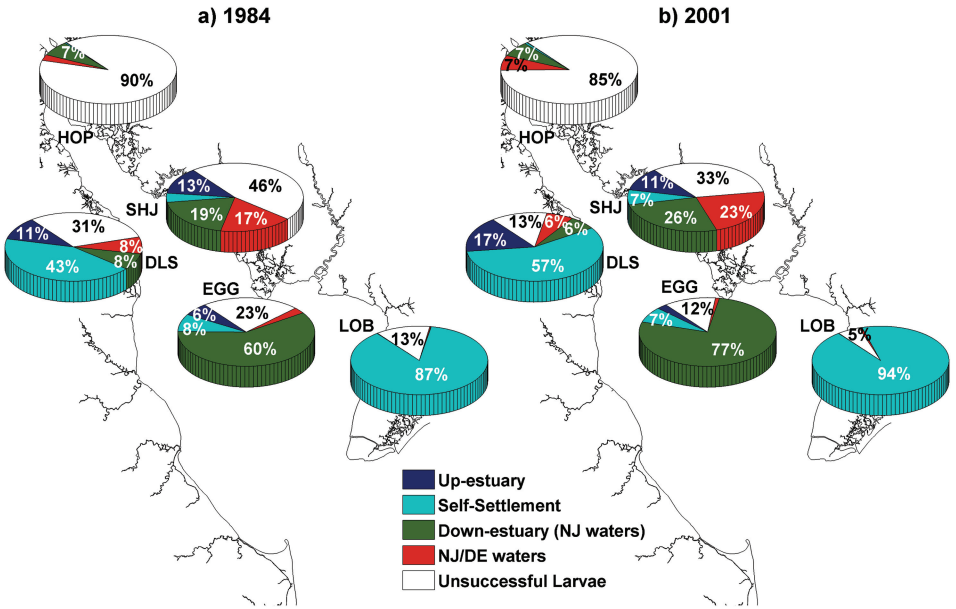


Figure 9. Fate of larvae released at Hope Creek (HOP), Ship John (SHJ), Egg Island (EGG), the Delaware side of the estuary (DLS), and the Lower Bay (LOB) during (a) low and (b) high river discharge conditions expressed as percent that are exported up-estuary, down-estuary, or settle locally. The across-estuary flux is estimated by the percent of particles that move from New Jersey to Delaware waters and vice versa (NJ/DE waters). The percent of unsuccessful larvae at each location is shown. Only values greater than 5% are shown.

had the highest success rates of 50–65% (Fig. 8). The Egg Island reef area is notable because larval success rates at this site were about one-half of those of the reef areas to the north and south, similar to Arnolds. Larval success was highest at all of the natural reef sites in 1986.

The general patterns of larval dispersal (Fig. 9) showed that the upper estuary had low larval success rates and a small percentage of larvae (~7%) were exported down-estuary from this region. Larvae spawned in the mid-estuary region along the New Jersey side remained in the area (self-settlement) or were exported down-estuary or across to the Delaware side of the estuary. Larvae spawned along the Delaware side had a higher potential of self-settlement (43–57%). The Egg Island region exported over half of its larvae to down-estuary regions. In the Lower Bay essentially all of the successful larvae recruited to the local region. High (1984) and low (2001) river discharge years showed essentially the same general dispersion patterns, but with increased success and transfer during low river discharge (Fig. 9a).

c. Evaluation of simulated larval dispersion patterns

The potential settlement pattern obtained from the simulated larval transfers (Fig. 7) was evaluated by comparisons with observed average oyster spat settlement (Fig. 10) and

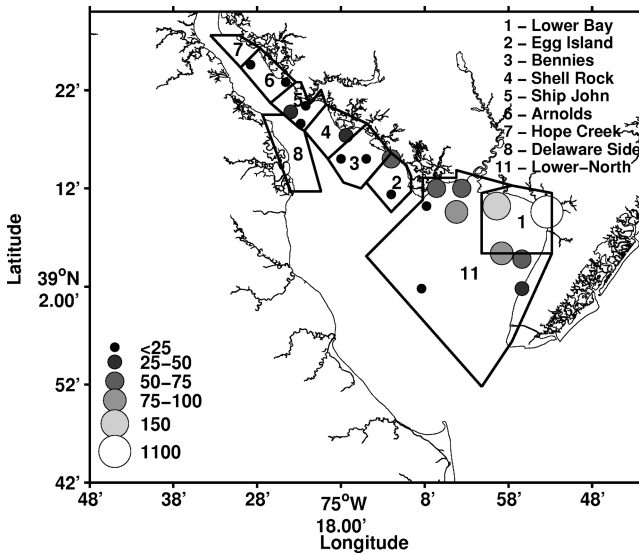


Figure 10. Oyster larvae settlement pattern obtained from spat set measurements made in Delaware Bay during the spawning season (June–October) from 1954–1986. The spawning season average mean cumulative spat per shell obtained from the measurements is indicated (dot size and color).

recruitment rates (Table 1). The oyster spat settlement sites were in the New Jersey waters of the estuary, so comparisons were made for only these areas. The observed settlement patterns (Fig. 10) showed low settlement in the upper estuary region around Arnolds oyster reef. Observed settlement increased down-estuary with the highest settlement occurring in the eastern-most part of the lower estuary adjacent to the Cape May Peninsula (Lower-North and Lower Bay regions in the simulations). The connectivity matrices show a similar pattern (Figs. 7 and 8). The highest simulated potential settlement rates were in the reef regions of the central and lower estuary, with the maximum simulated potential settlement in the Lower Bay region (Figs. 7, 8 and 9).

The observed recruitment patterns (Table 1) showed low recruitment in the upper estuary in the vicinity of Arnolds (a low mortality area, Powell *et al.*, 2008) and increased recruitment down-estuary toward Bennies oyster reef (a high mortality area, Powell *et al.*, 2008). In most years, the observed recruitment increased down-estuary, suggesting that the reefs in this region have a higher probability of successful recruitment. This down-estuary trend also occurred in the simulated larval success (Fig. 3c) and potential settlement (Fig. 7f) for most of the areas. However, Arnolds had the highest overall potential settlement but the lowest observed recruitment (Table 1). Part of this discrepancy may be attributed to the different areas that are used to calculate the potential settlement, which have regular shapes, versus the irregular shapes of the natural reefs. Also the model-based calculations do not include the small reefs that surround the larger reefs and the observations from the low mortality

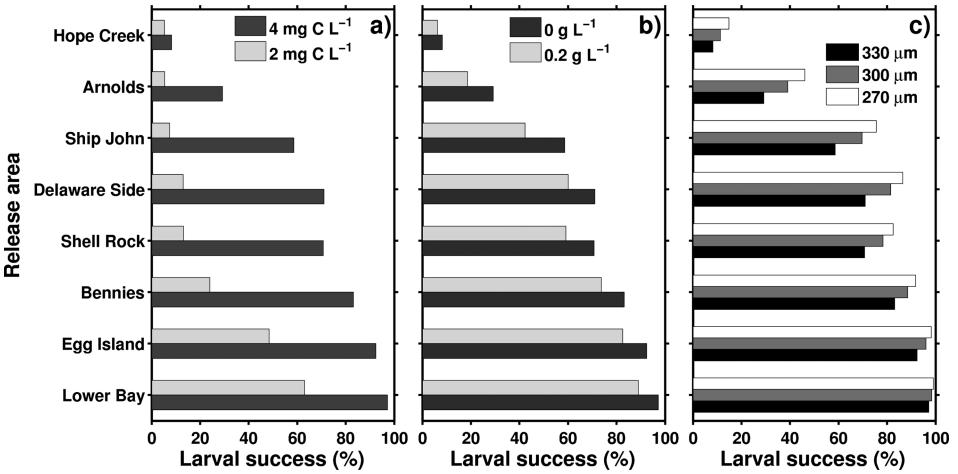


Figure 11. Percent of successful larvae for each release location that resulted from (a) decreased food concentration, (b) increased turbidity, and (c) decreased size at which settlement can occur. The percent larval success at each location obtained for the conditions used in the basic model simulations (filled bar) are shown for comparison.

areas include some upper estuary regions that have lower recruitment rates (Powell *et al.*, 2008), which might enhance differences with the simulated potential settlement.

The simulated potential settlement patterns generally reproduced the observed spatial variability in recruitment (Table 1) and settlement (Fig. 10), but year-to-year differences were not captured by the simulations. Some of the general trends in individual years were reproduced in the simulations, such as the higher observed recruitment and simulated potential settlement at Shell Rock and Bennies (Table 1). Also the lowest observed mean recruitment occurred in 1984 and 2001, and these years had the lowest overall mean potential settlement value (Table 1). However, the annual differences in simulated potential settlement were not of the same order of magnitude as the differences in the observed recruitment observations (Table 1). These differences indicate that processes other than simple delivery of larvae to a particular reef by the circulation are controlling recruitment to reefs in Delaware Bay.

d. Model sensitivity

Larval growth, success, and transfer are also dependent on food and turbidity concentrations and the choice made for the size at which a larva is competent to set (e.g., larval period duration). A reduction in food concentration from 4 to 2 mg C L⁻¹ decreased the simulated larval success for all of the release regions (Fig. 11a). From Hope Creek to Shell Rock, larval success was reduced to less than 20% of the success rates obtained with the higher food concentration. Success rates at sites in the lower estuary were higher, but still

less than those obtained with the higher food concentration. Even with the reduced food, an along-estuary gradient in larval success occurred.

The simulated larval success rates were not significantly changed by the inclusion of a moderate turbidity concentration (Fig. 11b). Success was reduced by 5–20%, with the largest reductions occurring in at the upper estuary regions. Setting at smaller size (i.e., shorter larval period duration) increased larval success rates, especially in the upper and middle regions of the estuary (Fig. 11c). The slower growing larvae in these regions have a higher survival with a smaller settlement size. The benefit of smaller settlement size was lost in the lower estuary, where success rate is essentially independent of settlement size (Fig. 11c).

6. Discussion and summary

a. Oyster larvae dispersion

The simulated transport patterns showed that larvae tended to drift down-estuary. This transport removes larvae from the upper estuary reefs and contributes to the reduced larval recruitment rate that has been observed for the up-estuary regions of Delaware Bay (Powell *et al.*, 2008). Down-estuary transport of larvae may be a basic pattern in estuarine systems. Modeling studies of oyster populations in Terrebonne Basin of south central Louisiana suggested that down-estuary transport occurred in this system (Soniati *et al.*, 1998).

The simulated particle trajectories showed that most larvae tended to remain in the release area or be transported to specific areas, especially in the middle and lower regions of the Delaware Bay. The simulated potential settlement patterns showed consistently higher rates of larval settlement in the lower estuary, which is in agreement with long-term observations from Delaware Bay (Table 1, Fig. 10). The particle trajectories showed that larvae originating from the Lower Bay reef support higher potential settlement in the lower estuary. The topography of the lower estuary forms a shallow semi-enclosed region behind the Cape May Peninsula (Fig. 1). This area is characterized by a high retention of passive particles, suggesting a recirculating flow and weak currents (Narváez *et al.*, this issue). Thus, the circulation in the lower Delaware Bay may maintain the high rates of self-settlement in this area.

The oyster reefs along the Delaware side of the estuary also showed the potential of being supported by self-settlement. The freshwater plume from the Delaware River exits the estuary along the Delaware side (Galperin and Mellor, 1990; Whitney and Garvine, 2006), which provides a consistent out-estuary flow that is enhanced during periods of high river discharge ($>500 \text{ m}^3 \text{ s}^{-1}$). A consistent outflow potentially supports horizontal dispersal, but the high potential self-settlement and low exchange with nearby regions indicated by the particle transport patterns suggest low across-estuary transport and low net dispersal (Fig. 9). Larval supply from the natural reefs on the New Jersey side to the Delaware side of the estuary tends to be from the middle estuary reefs areas (Ship John to Bennies), although

this is a small contribution to the overall recruitment to reefs on the Delaware side of the estuary.

Low rates of across-estuary dispersal of eastern oyster larvae have been observed in other estuarine systems. Observations from Mobile Bay, Alabama showed an across-estuary gradient in eastern oyster larvae, with regions of high settlement in the western bay (Kim *et al.*, 2010 and references therein). Lagrangian particle tracking simulations implemented for Mobile Bay showed a decreasing west to east gradient in eastern oyster larvae supply that was supported by local settlement that was maintained by the circulation (Kim *et al.*, 2010). In contrast, North *et al.* (2008) found that eastern oyster larvae in the upper Chesapeake Bay dispersed away from their natal populations with low self-settlement rates.

The Delaware Bay simulations showed that periods of low river discharge were characterized by the availability of more larvae throughout the estuary, potentially increasing the probability of encountering good habitat for settlement. North *et al.* (2008) showed that eastern oyster larvae in Chesapeake Bay had a higher chance of encountering a suitable settlement habitat during periods of low river discharge. Thus, enhanced growth rate, shorter planktonic larval duration, more overall larvae, and reduced down-estuary transport should support increased larval success in years characterized by reduced river discharge. However, this prediction is independent of the post-settlement populations (the source of the larvae), which may experience increased disease mortality during periods of high salinity (see Bushek *et al.* and Ford *et al.*, this issue).

b. Model limitations

The potential settlement of the simulated larval particles was based on reaching a particular settlement size. In nature, biological and physical cues, such as the presence of adult oysters and the availability of clean substrate, are known to initiate and encourage larval settlement (e.g., Osman *et al.*, 1989; Roegner and Mann, 1990; Fitt and Coon, 1992). The settlement criteria used in the model assumed that these cues might be equivalent throughout Delaware Bay. The general agreement between the simulated settlement patterns and the observed along-estuary recruitment pattern (Table 1, Fig. 10) supports the assumption that variability in these cues is not a significant determinant of larval settlement patterns in Delaware Bay. Also, variations in larval settlement size did not significantly alter the overall settlement patterns obtained from the simulations. These results support the coupled modeling approach as being adequate for obtaining basic spatial patterns of oyster larvae settlement in Delaware Bay.

The mortality that resulted in the simulated larval success rates of 50–60% was produced primarily by low salinity and to a lesser extent cooler temperature. Predation mortality was not included as a loss for larvae during the planktonic transport phase, although this is potentially an important process (Deksheniaks *et al.*, 1997). Predation pressure depends on larval size and location in the water column (Deksheniaks *et al.*, 1997) and insufficient information is available from Delaware Bay to estimate the contribution of these losses.

The number of simulated particles used in this study represents a small fraction of the larvae that are released by the post-settlement oyster population during the spawning season. Simulations in which particles were released in proportion to the estimated oyster population at individual reefs (Powell *et al.*, 2008) using conditions from 1985 and 2000 showed larval success and dispersion patterns that were similar to those obtained by releasing the same number of particles from each area. The implication is that the circulation and larval growth might be more important than the total number of individuals spawned, in determining larval dispersal patterns in Delaware Bay. Thus, an accurate representation of physical (circulation) and biological (larval growth) processes is critical to understanding eastern oyster larvae success and settlement patterns.

The general simulated potential settlement patterns were similar to the observed recruitment patterns, but specific years showed differences that were not captured by the simulations. Differences in what is represented by the observed recruitment rates and simulated potential settlement values may explain some of these discrepancies. Also, the use of a prescribed food supply potentially contributes to differences in observed and simulated settlement patterns. Variability in the timing and quality of the food supply can have significant effects on oyster larvae success (Bochenek *et al.*, 2001; Hofmann *et al.*, 2004). Including more realistic food distributions and accounting for planktonic and post-settlement predation mortality will allow more accurate projections of temporal and spatial variability in the recruitment of eastern oyster larvae in Delaware Bay.

c. Implications for Delaware Bay oyster population

Of the variables tested with the Lagrangian particle simulations, the along-estuary salinity distribution was the primary determinant of simulated oyster larvae success in Delaware Bay. The potential settlement for larvae released in the upper estuary was less than half that of larvae originating in the lower estuary because of the detrimental effect of low salinity on simulated larval growth. Periods of high river discharge further reduced potential settlement, especially when the low salinity conditions were extended in space and time. The mid-Atlantic portion of the United States is expected to experience wetter conditions and increased river discharge as a result of a warming climate (Najjar *et al.*, 2000, 2009; IPCC, 2007). Thus, expansion of the low salinity portions of Delaware Bay may reduce oyster larvae growth and success and limit the regions that sustain the natural oyster reefs.

The simulated transport patterns showed that oyster larvae tend to drift down-estuary during the spawning season, which can produce extensive mixing of the larvae throughout Delaware Bay. This model-based result is consistent with the analysis presented in He *et al.* (this issue) that shows that most of the oysters in the main region of Delaware Bay are genetically homogeneous. Also, the simulated dispersal patterns of oyster larvae originating from some of the reefs in the middle and lower regions of Delaware Bay show considerable self-settlement, which may contribute to a genetically homogeneous oyster population. Mixing of larvae spawned in the upper reaches of the estuary is limited, in part because

of the lower overall survival in the low salinity regions. Oysters in the upper estuary have been shown to be genetically different from those in the middle and lower estuary (He *et al.*, this issue), which suggests little exchange. The simulated transport patterns showed that the upper estuary exports rather than receives larvae. This has implications for the establishment of genetic characteristics, such as disease resistance, and for the maintenance of oyster populations that are susceptible to diseases (Hofmann *et al.*, 2009; Ford *et al.*, this issue; Wang *et al.*, this issue).

The circulation of the Delaware Bay estuary is critical to the patterns of larval dispersal. Changes in atmospheric forcing and freshwater inflow can alter the estuary circulation, which in turn can modify dispersal and potential settlement patterns of oyster larvae in Delaware Bay. Addressing the consequences of such modifications should be a component of management strategies and policies that are developed for Delaware Bay oyster populations.

Acknowledgments. We thank Hernan Arango for help in coupling the oyster larvae growth and behavior models to ROMS. Zhiren Wang provided the circulation model configuration files. Kathryn Ashton-Alcox and Susan Ford provided the observations of Delaware Bay oyster recruitment. The constructive comments from the editor, Kenneth Brink, and three anonymous reviewers are appreciated. Support for this research was provided by the National Science Foundation Ecology of Infectious Diseases Program through grant OCE-06-22642.

REFERENCES

- Andrews, J. D. 1983. Transport of bivalve larvae in James River, Virginia. *J. Shellfish Res.*, 3, 29–40.
- Bochenek, E. A., J. M. Klinck, E. N. Powell and E. E. Hofmann. 2001. A biochemically based model of the growth and development of *Crassostrea gigas* larvae. *J. Shellfish Res.*, 20, 243–265.
- Bushek, D., S. E. Ford and I. Burt. 2012. Long-term patterns of an estuarine pathogen along a salinity gradient. *J. Mar. Res.*, 70, 225–251.
- Carriker, M. R. 1951. Ecological observations on the distribution of oyster larvae in New Jersey estuaries. *Ecol. Monogr.*, 21, 19–38.
- Cook, T. L., C. K. Sommerfield and K.-C. Wong. 2007. Observations of tidal and springtime sediment transport in the upper Delaware Estuary. *Estuar. Coast. Shelf Sci.*, 72, 235–246, doi:10.1016/j.ecss.2006.10.014.
- Davis, H. C. 1958. Survival and growth of clam and oyster larvae at different salinities. *Biol. Bull.*, 114, 296–307.
- 1960. Effects of turbidity-producing materials in sea water on eggs and larvae of the clam (*Venus mercenaria mercenaria*). *Biol. Bull.*, 118, 48–54.
- Davis, H. C. and A. Calabrese. 1964. Combined effects of temperature and salinity on the development of eggs and growth of larvae of *Mercenaria mercenaria* and *Crassostrea virginica*. *Fish Bull.*, 63, 643–655.
- Dekshenieks, M. M., E. E. Hofmann, J. M. Klinck and E. N. Powell. 1996. Modeling the vertical distribution of oyster larvae in response to environmental conditions. *Mar. Ecol. Prog. Ser.*, 136, 97–110.
- 1997. A modeling study of the effects of size- and depth-dependent predation on larval survival. *J. Plankton Res.*, 19, 1583–1598.

- Deksheniaks, M. M., E. E. Hofmann and E. N. Powell. 1993. Environmental effects on the growth and development of eastern oyster, *Crassostrea virginica* (Gmelin, 1791), larvae: A modeling study. *J. Shellfish Res.*, 12, 241–254.
- Emery W. J. and R. E. Thomson. 2001. *Data Analysis Methods in Physical Oceanography*, Elsevier, 638 pp.
- Fegley, S. R., S. E. Ford, J. N. Kraeuter and H. H. Haskin. 2003. The persistence of New Jersey's oyster seedbeds in the presence of oyster disease and harvest: the role of management. *J. Shellfish Res.*, 22, 451–464.
- Fitt, W. K. and S. L. Coon. 1992. Evidence for ammonia as a natural cue for recruitment of oyster larvae to oyster beds in a Georgia salt marsh. *Biol. Bull.*, 182, 401–408.
- Ford, S. E., E. Scarpa and D. Bushek. 2012. Spatial and temporal variability of disease refuges in an estuary: Implications for the development of resistance. *J. Mar. Res.*, 70, 253–277.
- Galperin, B. and G. L. Mellor. 1990. A time-dependant, three-dimensional model of the Delaware Bay and River system. Part 2: Three-dimensional flow fields and residual circulation. *Estuar. Coast. Shelf Sci.*, 31, 255–281.
- Garvine, R. W. 1991. Subtidal frequency estuary-shelf interaction: Observations near Delaware Bay. *J. Geophys. Res.*, 96, 7049–7064.
- Garvine, R. W., R. K. McCarthy and K.-C. Wong. 1992. The axial salinity distribution in the Delaware Estuary and its weak response to river discharge. *Estuar. Coast. Shelf Sci.*, 35, 157–165.
- Hamming, R.W. 1959. Stable predictor-corrector methods for ordinary differential equations. *J. Assoc. Comp. Math.*, 6, 37–47.
- Haskin, H. H. and S. E. Ford. 1982. *Haplosporidium nelsoni* (MSX) on Delaware Bay seed oyster beds: a host-parasite relationship along a salinity gradient. *J. Invert. Pathol.*, 40, 388–405.
- He, Y., S. E. Ford, D. Bushek, E. N. Powell, Z. Bao and X. Guo. 2012. Effective population sizes of eastern oyster *Crassostrea virginica* (Gmelin) populations in Delaware Bay, USA. *J. Mar. Res.*, 70, 357–379.
- Hidu, H and H. H. Haskin. 1978. Swimming speeds of oyster larvae *Crassostrea virginica* in different salinities and temperatures. *Estuaries*, 1, 252–255.
- Hofmann, E. E, D. Bushek, S. E. Ford, X. Guo, D. Haidvogel, D. Hedgecock, J. M. Klinck, C. Milbury, D. A. Narváez, E. N. Powell, Y. Wang, Z. Wang, J. Wilkin and L. Zhang. 2009. Understanding how disease and environment combine to structure resistant in estuarine bivalve populations. *Oceanography*, 22, 212–231.
- Hofmann, E. E, E. N. Powell, E. A. Bochenek and J. M. Klinck. 2004. A modeling study of the influence of environment and food supply on survival of *Crassostrea gigas* larvae. *ICES J. Mar. Sci.*, 61, 596–616.
- Hunter, J., P. Craig and H. Phillips. 1993. On the use of random walk models with spatially variable diffusivity. *J. Comput. Phys.*, 106, 366–376.
- IPCC. 2007. Summary for policymakers, in *Climate change 2007: The Physical Science Basis, Contribution of Working Group I to the Fourth Assessment Report of the Intergovernmental Panel on Climate Change*, S. Solomon, D. Qin, M. Manning, Z. Chen, M. Marquis, K. B. Averyt, M. Tignor, H. L. Miller, eds., Cambridge University Press, Cambridge, United Kingdom and New York, NY, USA, 996 pp.
- Jacobsen, T. R., J. D. Milutinovic and J. R. Miller. 1990. Observational and model studies of physical processes affecting benthic larval recruitment in Delaware Bay. *J. Geophys. Res.*, 95, 20331–20345.
- Kennedy, V. S. 1996. Biology of larvae and spat, in *The Eastern Oyster, Crassostrea virginica*, V. S. Kennedy, R. I. E. Newell and A. F. Eble, eds., Maryland Sea Grant, 371–411.
- Kennedy, V. S. and W. F. Van Heukelem. 1986. Responses to environmental factors by larval oysters (*Crassostrea virginica*). *Am. Malac. Bull.*, 4, 101.

- Kim, C.-K., K. Park, S. P. Powers, W. M. Graham and K. M. Bayha. 2010. Oyster larval transport in coastal Alabama: Dominance of physical transport over biological behavior in a shallow estuary. *J. Geophys. Res.*, *115*, C10019, doi:10.1029/2010JC006115.
- Kraeuter, J. N., S. E. Ford and W. Canzonier. 2003. Increased biomass yield from Delaware Bay oysters (*Crassostrea virginica*) by alteration of planting season. *J. Shellfish Res.*, *22*, 39–49.
- Kraeuter, J. N., S. E. Ford and M. Cummings. 2007. Oyster growth analysis: a comparison of methods. *J. Shellfish Res.*, *26*, 479–491.
- MacKenzie Jr., C. L. 1996. History of oystering in the United States and Canada, featuring the eight greatest oyster estuaries. *Mar. Fish. Rev.*, *58*, 1–78.
- Marchesiello, P., J. C. McWilliams and A. F. Shchepetkin. 2001. Open boundary conditions for long-term integration of regional ocean models. *Ocean Model.*, *3*, 1–20.
- Mesinger, F., G. DiMego, E. Kalnay, K. Mitchell, P. C. Shafran, W. Ebisuzaki, D. Jovic, J. Woolen, E. Rogers, E. H. Berbery, M. B. Ek, Y. Fan, R. Grumbine, W. Higgins, H. Li, Y. Lin, G. Manikin, D. Parrish and W. Shi. 2006. North American regional reanalysis. *Bull. Am. Meteorol. Soc.*, *87*, 343–360.
- Mukai, A. Y., J. J. Westerink, R. A. Luettich and D. Mark. 2002. Eastcoast 2001, A tidal constituent database for the western North Atlantic, Gulf of Mexico and Caribbean Sea, Tech. Rep. ERDC/CHL TR-02-24, 196 pp.
- Najjar R. G., L. Patterson and S. Graham. 2009. Climate simulations of major estuarine watersheds in the Mid-Atlantic region of the United States. *Climatic Change*, *95*, 139–168.
- Najjar, R. G., H. A. Walker, P. J. Anderson, E. J. Barron, R. J. Bord, J. R. Gibson, V. S. Kennedy, C. G. Knight, J. P. Megonigal, R. E. O'Connor, C. D. Polsky, N. P. Psuty, B. Richards, L. G. Sorenson, E. M. Steele and R. S. Swanson. 2000. The potential impacts of climate change on the Mid-Atlantic Coastal Region. *Clim. Res.*, *14*, 219–233.
- Narváez, Diego A., John M. Klinck, Eric N. Powell, Eileen E. Hofmann, John Wilkin and Dale B. Haidvogel. 2012. Circulation and behavior controls on dispersal of eastern oyster (*Crassostrea virginica*) larvae in Delaware Bay. *J. Mar. Res.*, *70*, 411–440.
- North, E. W., Z. Schlag, R. R. Hood, M. Li, L. Zhong, T. Gross and V. S. Kennedy. 2008. Vertical swimming behavior influences the dispersal of simulated oyster larvae in a coupled particle-tracking and hydrodynamic model of Chesapeake Bay. *Mar. Ecol. Prog. Ser.*, *359*, 99–115.
- Osman, R. W., R. B. Whitlatch and R. N. Zajac. 1989. Effects of resident species on recruitment into a community: larval settlement versus post-settlement mortality in the oyster *Crassostrea virginica*. *Mar. Ecol. Prog. Ser.*, *54*, 61–73.
- Powell, E. N., K. A. Ashton-Alcox, J. N. Kraeuter, S. E. Ford and D. Bushek. 2008. Long-term trends in oyster population dynamics in Delaware Bay: regime shifts and response to disease. *J. Shellfish Res.*, *27*, 729–755.
- Powell, E. N., J. M. Klinck, E. E. Hofmann and S. E. Ford, 1997. Varying the timing of oyster transplant: implications for management from simulation studies. *Fish. Oceanogr.*, *6*, 213–237.
- Powell, E. N., D. A. Kreeger, J. M. Morson, D. B. Haidvogel, Z. Wang, R. Thomas and J. E. Gius. 2012. Oyster food supply in Delaware Bay: Estimation from a hydrodynamic model and interaction with the oyster population. *J. Mar. Res.*, *70*, 469–503.
- Rhodes, E. W. and W. S. Landers. 1973. Growth of oyster larvae, *Crassostrea virginica*, of various sizes in different concentrations of the chrysophyte, *Isochrysis galbana*. *Proc. Natl. Shellfish Ass.*, *63*, 53–59.
- Roegner, G. C. and R. Mann. 1990. Settlement patterns of *Crassostrea virginica* (Gmelin, 1791) larvae in relation to tidal zonation. *J. Shellfish Res.*, *9*, 341–346.
- Sharp, J. H., L. A. Cifuentes, R. B. Coffin and J. R. Pennock. 1986. The influence of river variability on the circulation, chemistry, and microbiology of the Delaware Estuary. *Estuaries*, *9*, 261–269.

- Shchepetkin, A. F. and J. C. McWilliams. 2005. The Regional Ocean Modeling System (ROMS): A split-explicit, free-surface, topography-following coordinates ocean model. *Ocean Model.*, 9, 347–404.
- Soniat, T. M., E. N. Powell, E. E. Hofmann and J. M. Klinck. 1998. Understanding the success and failure of oyster populations: the importance of sampled variables and sample timing. *J. Shellfish Res.*, 17, 1149–1165.
- Thompson, R. J., R. I. E. Newell, V. S. Kennedy and R. Mann. 1996. Reproductive processes and early development, in *The Eastern Oyster, Crassostrea virginica*, V. S. Kennedy, R. I. E. Newell and A. F. Eble, eds., Maryland Sea Grant, 371–411.
- Visser, A. W. 1997. Using random walk models to simulate the vertical distribution of particles in a turbulent water column. *Mar. Ecol. Prog. Ser.*, 158, 275–281.
- Walters, R. A. 1997. A model study of tidal and residual flow in Delaware Bay and River. *J. Geophys. Res.*, 102, 12689–12704.
- Wang, Z., D. Haidvogel, D. Bushek, S. E. Ford, E. E. Hofmann, E. N. Powell and J. Wilkin. 2012. Circulation and water properties and their relationship to the oyster disease, MSX, in Delaware Bay. *J. Mar. Res.*, 70, 279–308.
- Whitney, M. M. and R. W. Garvine. 2006. Simulating the Delaware Bay buoyant outflow: Comparison with observations. *J. Phys. Oceanogr.*, 36, 3–21.
- Wong, K.-C. 1994. On the nature of transverse variability in a coastal plain estuary. *J. Geophys. Res.*, 99, 14209–14222.
- Wong, K.-C. and R. W. Garvine. 1984. Observations of wind-induced, subtidal variability in the Delaware estuary. *J. Geophys. Res.*, 89(C6), 10589–10597.

Received: 24 October, 2011; revised: 19 July, 2012.